ACS chemical biology

Letters

pubs.acs.org/acschemicalbiology

Rapidly Relocating Molecules Between Organelles to Manipulate Small GTPase Activity

Siew Cheng Phua,[†] Christopher Pohlmeyer,[†] and Takanari Inoue*[,†,‡]

[†]Department of Cell Biology, Center for Cell Dynamics, Johns Hopkins University, Baltimore, Maryland 21205, United States

[‡]PRESTO Investigator, JST, 4-1-8 Honcho Kawaguchi, Saitama 332-0012, Japan

Supporting Information

ABSTRACT: Chemically inducible rapid manipulation of small GTPase activity has proven a powerful approach to dissect complex spatiotemporal signaling of these molecular switches. However, overexpression of these synthetic molecular probes freely in the cytosol often results in elevated background activity before chemical induction, which perturbs the cellular basal state and thereby limits their wide application. As a fundamental solution, we have rationally designed and newly developed a strategy to remove unwanted background activity without compromising the extent of induced activation. By exploiting interaction between a membrane lipid and its binding protein, target proteins were translocated from one organelle to another on a time scale of seconds. This improved strategy now allows for rapid manipulation of small GTPases under a physiological state, thus enabling fine dissection of sophisticated signaling processes shaped by these molecules.

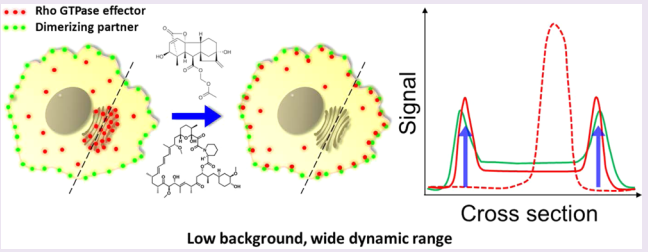

We have previously developed a series of molecular probes based on a chemically inducible heterodimerization strategy, which enabled activation or inactivation of Rho family members of small GTPases in living cells on a time scale of seconds.[1,2] This strategy has been extended to other members, such as Ras[3] and Arf6,[4] and also provided high spatial control where a light sensitive dimerizer was used.[5,6] In these methods, a chemical dimerizer, either rapamycin or gibberellin, induces the rapid translocation of cytosolic FKBP- or GID1-fused GTPases (or GTPase effectors) to the plasma membrane, where the respective dimerizing partner, FRB or GAI, is localized (Figure 1a).[1,2] Thus, the addition of the chemical dimerizer concentrates cytosolic effectors at the plasma membrane by a factor of 500 to 1000 for a typical mammalian cell. This rapid and significant chemically inducible concentration triggers activation of Rho GTPases and downstream signaling at the cell periphery, resulting in membrane ruffling and c-Jun N-terminal kinase activation.[1,2]

Despite its power and utility, this technique has an inherent limitation; unwanted target activation of varying extent is frequently exhibited in the absence of chemical dimerizers. This happens because cytosolic dimerizing effectors still have access to the plasma membrane as a consequence of free diffusion (Figure 1b). For useful application in spatiotemporal signaling studies, it is critical to keep such background activity as low as possible to achieve high efficiency in inducible translocation and/or activation. Therefore, we aimed to restrict the free diffusion of dimerizing effector molecules in the cytosol. One could think of confining these effector molecules inside the cell nucleus until rapamycin is added.[7] However, this approach results in slower onset of target activation as the nuclear export process is an additional step before effectors can be trapped at the plasma membrane.

To avoid this additional step, we employed a binding protein for a Golgi membrane lipid to tether FKBP-fused GTPase effector molecules onto the cytoplasmic surface of the Golgi apparatus in the uninduced basal state (Figure 1c). A family of four-phosphate-adaptor proteins (FAPPs) binds to the phosphatidylinositol 4-phosphate (PI4P) lipid enriched at the trans-Golgi network through their pleckstrin homology (PH) domains.[8] Specifically, FAPP1 has been reported to bind to PI4P with a dissociation constant of 230 nM.[9] It may thus be expected that, while most of the FKBP effectors fused with the PH(FAPP) domain would remain on the Golgi surface at any given time, these molecules would essentially display dynamic binding behavior by dissociating from the Golgi surface and freely diffuse in the cytosol before reassociating with PI4P. When rapamycin is present, however, these FKBP effector molecules bind to rapamycin with a K_d of 0.2 nM,[10] and those that are diffusing in the cytosol at a given time may subsequently get trapped by the FRB anchored at the plasma membrane. Since the FKBP.rapamycin binary complex binds to FRB (K_d = 12 nM[10]) with an approximately 20-fold higher binding affinity than the PH(FAPP).PI4P interaction, an assumption is made that the FKBP effectors are more likely to be kept at the plasma membrane than return to the Golgi surface in the presence of rapamycin.

Received: June 5, 2012
Accepted: September 21, 2012
Published: September 21, 2012

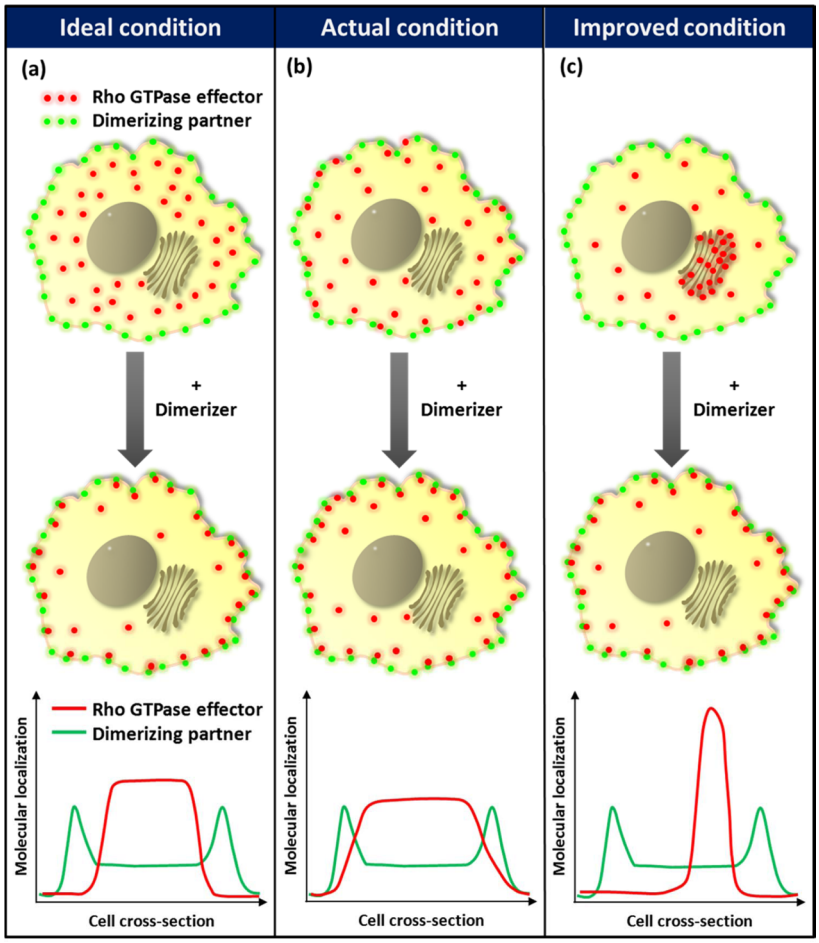

Figure 1. Schematic of the present chemically inducible heterodimerization strategy and the corresponding improved strategy. (a) Under ideal conditions, cytosolic GTPase effectors only diffuse and bind to plasma membrane dimerizing partners upon the addition of dimerizer (b) The present strategy is limited by the random diffusion of cytosolic GTPase effectors to the cell cortex and plasma membrane, resulting in background activity in the absence of dimerizer. (c) Background activity may be reduced by tethering GTPase effectors to cytosolic organelles to limit the random diffusion. The graphs at the bottom of each panel illustrate the localization of GTPase effectors relative to the plasma membrane-tethered dimerizing partner in the uninduced state.

In this study, we have manipulated the activity of small GTPase Rac1 via Tiam1, a guanine nucleotide exchange factor of Rac1. To test our ideas, we first generated a fusion protein of PH(FAPP1) and FKBP-Tiam1 with a mCherry tag (PH-(FAPP1)-mCherry-FKBP-Tiam1; PMFT) (Figure 2a).We then transfected PH(FAPP1)-mCherry-FKBP-Tiam1 in Cos-7 cells together with Lyn-GFP-FRB (LGR; a plasma membrane targeted FRB labeled with GFP). Line scan analysis confirmed that PH(FAPP) efficiently localized PH(FAPP1)-mCherry-FKBP-Tiam1 to the Golgi, while mCherry-FKBP(MF) and mCherry-FKBP-Tiam1(MFT) are dispersed in the cytosol (Figure 2b and Supplementary Figure 1). Localization of Tiam1 to the Golgi did not appear to have any obvious effect on the Golgi structure; and quantification of the Golgi extent[11] in all three types of cells also yielded comparable results (Supplementary Figure 2). Furthermore, subsequent addition of rapamycin induced rapid translocation of PH(FAPP1)-mCherry-FKBP-Tiam1 to the plasma membrane (Figure 2biii and Supplementary Figures 3 and 4iii). We analyzed the translocation kinetics by measuring the mCherry fluorescent intensity at the Golgi (Figure 2ciii), finding 27.9 s to achieve the half-maximal translocation. This kinetics is comparably fast to what was achieved by cytosolic mCherry-FKBP (11.9 s) and mCherry-FKBP-Tiam1 (17.5 s) (Figure 2ci,ii and Supplementary Figure 4ci,ii). At 5 min post- rapamycin addition, translocation approaches saturation, and the average PH-(FAPP1)-mCherry-FKBP-Tiam1 Golgi signal diminished to 57% of the initial signal intensity, indicating that approximately 43% of the molecules have translocated away from the Golgi toward the plasma membrane (Figure 2ciii). In addition, PH(FAPP1)-mCherry-FKBP-Tiam1 stayed at the plasma membrane for at least 20 min and did not go back to the Golgi (Figure 3aiii). These data well supported our initial ideas: (1) the PH(FAPP1).PI4P interaction is sufficiently strong to localize PH(FAPP1)-mCherry-FKBP-Tiam1 at the Golgi and (2) the 20-fold stronger binding interaction between FKBP.rapamycin complex and FRB is highly efficient in recruiting Tiam1 and overcoming the reassociation of PH-(FAPP1) and PI4P.

We then compared the biological effect of the Golgi- and cytosol-localized Tiam1. Since translocation of Tiam1 to the plasma membrane promotes the local activation of Rac1 to result in membrane ruffling, we employed a semiquantitative method to score membrane ruffling activity (see Methods and Supplementary Table S1 for quantification method).[2,12] Control cells expressing mCherry-FKBP with Lyn-GFP-FRB

dx.doi.org/10.1021/cb300280k | ACS Chem. Biol. 2012, 7, 1950−1955

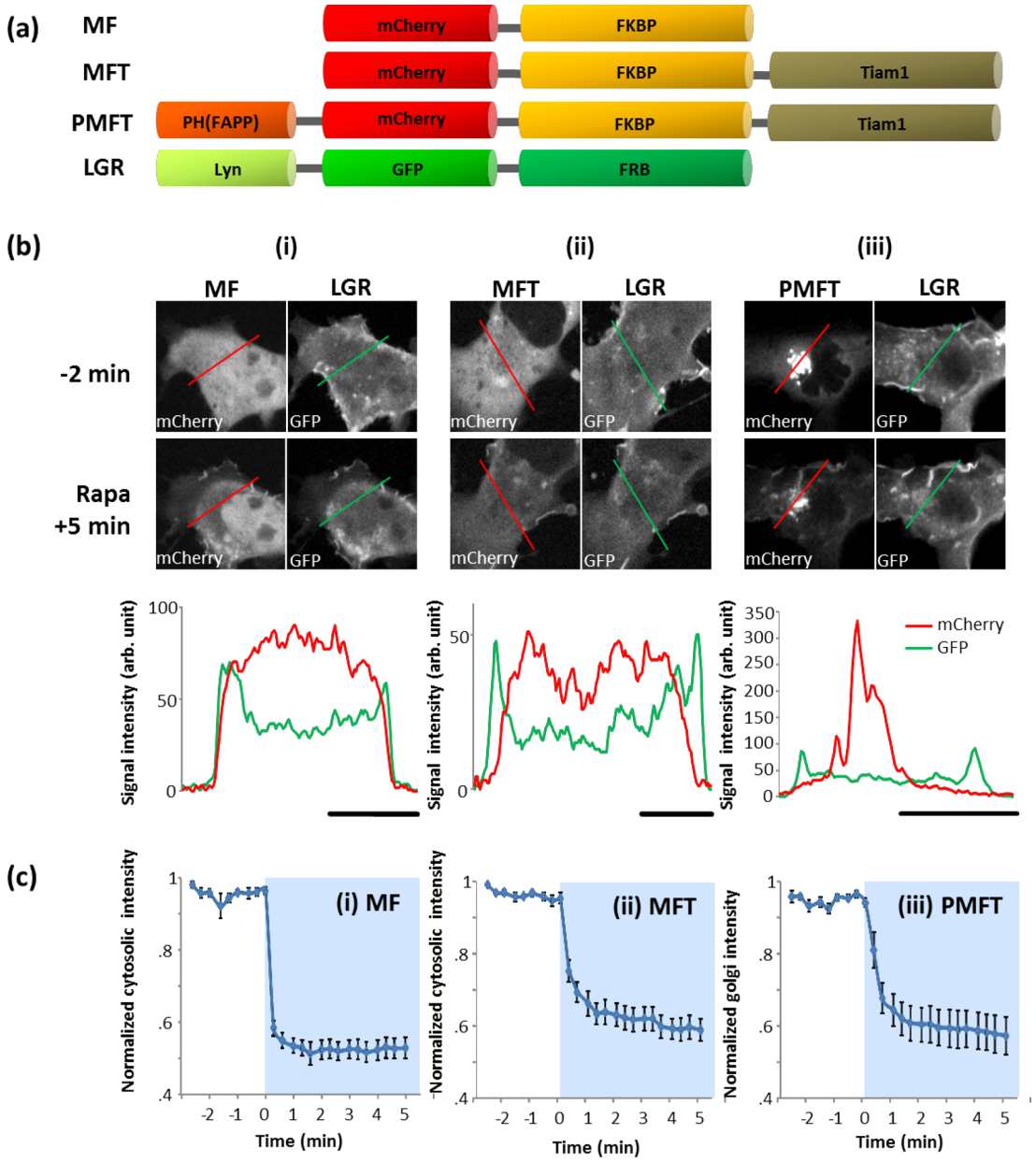

Figure 2. Localization and translocation of PH(FAPP1)-mCherry-FKBP-Tiam1 at the Golgi (a) Schematic representation of the various FKBP-fused Tiam1 constructs (MFT and PMFT), control construct (MF), and plasma membrane tethered Lyn-GFP-FRB (LGR) construct. (b) Confocal fluorescent images showing the cellular localization of (i) MF, (ii) MFT, or (iii) PMFT with LGR at defined time points before (−) and after (+) rapamycin addition. Graph at the bottom of each column is a line scan of the respective cells *prior* to rapamycin addition (from respective red and green lines drawn on top panel cell images). Note that the LGR signal intensities are comparable in i−iii. Scale bar beneath each graph represents 10 μm. (c) Average translocation kinetics of (i) MF, (ii) MFT, or (iii) PMFT from the cytosol or Golgi (note *y*-axis), where light blue regions indicate the presence of rapamycin. Signal intensities have been normalized against the maximum signal intensity values in each case. The average duration for MF, MFT, and PMFT to reach half-maximal translocation were 11.9, 17.5, and 27.9 s, respectively. SEM values are indicated by error bars.

exhibited low levels of membrane ruffling (median = 1), which did not alter after recruitment of mCherry-FKBP to the plasma membrane upon rapamycin addition (median = 1, p = 0.730) (Figures 3ai,b and Supplementary Video 1). All statistical values are summarized in Supplementary Table S2. In contrast, cells expressing cytoplasmic mCherry-FKBP-Tiam1 with Lyn-GFP-FRB already exhibited significantly higher levels of membrane ruffling (median = 2; MF− vs MFT−, p = 0.00969) in the uninduced state. The ruffling activity was further increased after rapamycin-mediated translocation of mCherry-FKBP-Tiam1 to the plasma membrane (median = 3, p = 0.000275) (Figure 3aii,b and Supplementary Video 2). Importantly, the Golgi confinement of PH(FAPP1)-mCherry-FKBP-Tiam1 exhibited significantly low levels of membrane ruffling (median = 1) in the uninduced state, comparable to that of the control condition (MF− vs PMFT−, p = 0.917) and significantly lower than that of mCherry-FKBP-Tiam1 (MFT− vs PMFT−, p = 0.0156) (Figure 3aiii,b). Upon rapamycin addition, PH(FAPP1)-mCherry-FKBP-Tiam1 expressing cells induced striking ruffling activity with a median score of 3, comparable to that of mCherry-FKBP-Tiam1 (MFT+ vs PMFT+, p = 0.190) (Figure 3aiii,b and Supplementary Video 3). Collectively, these data showed that Golgi sequestration of Tiam1 almost completely removes unwanted membrane ruffling activity in

dx.doi.org/10.1021/cb300280k | *ACS Chem. Biol.* 2012, 7, 1950−1955

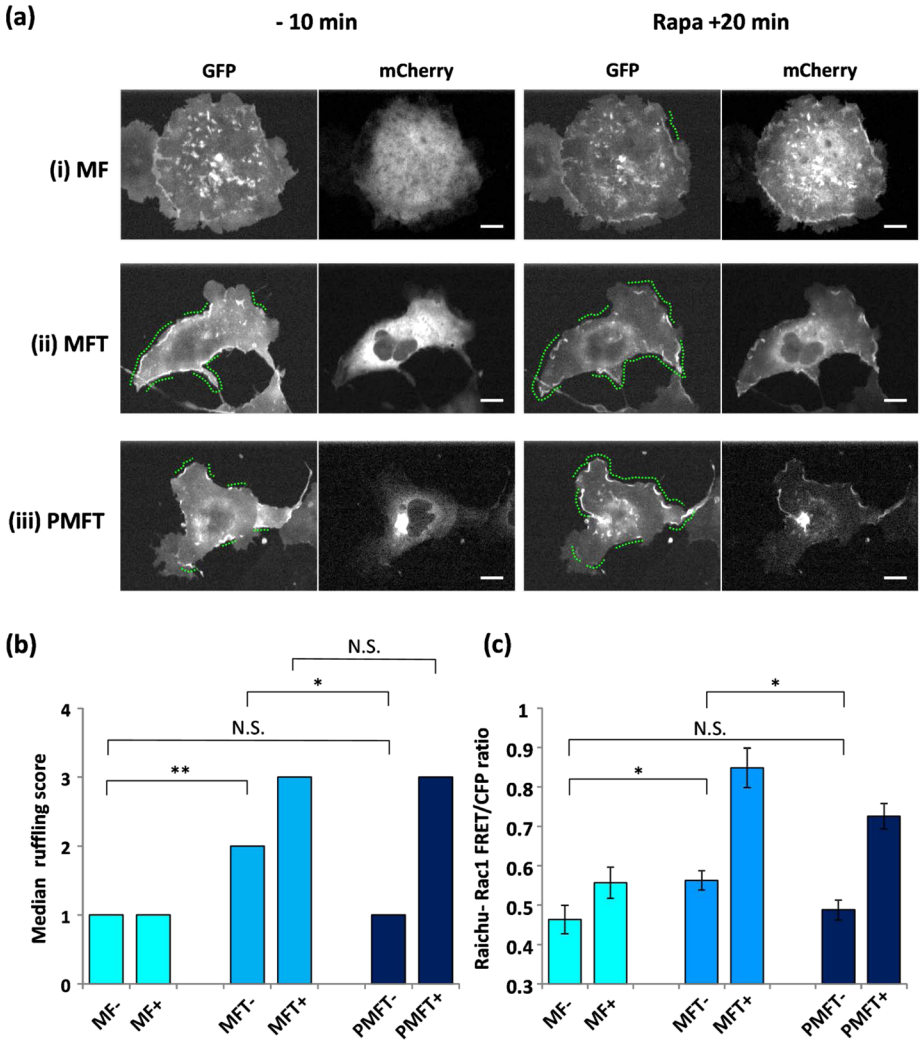

Figure 3. Membrane ruffling analysis and quantitative comparison of Rac1 activation levels in cells. (a) Confocal fluorescent images of cells expressing (i) MF(mCherry), (ii) MFT(mCherry), or (iii) PMFT(mCherry) with LGR (GFP) at defined time points before (−) and after (+) rapamycin addition. Green dotted lines on GFP images indicate regions of cellular edge displaying membrane ruffling activity during the 10 min before and 20 min after rapamycin addition. Scale bar indicates 10 μm. (b) Using the scoring scheme in Supplementary Table 1, cells expressing MF, MFT, and PMFT were scored for membrane ruffling levels before (−) and after (+) rapamycin addition. Median membrane ruffling level for each sample is shown. p values from two-tailed Mann−Whitney U tests between different samples are also represented. (c) Rac1 activity levels represented by FRET/CFP ratios in cells expressing MF, MFT, or PMFT with Lyn-linker-FRB (LDR) and RaichuEV-Rac1 FRET biosensor before and after 7 min of rapamycin treatment. Average FRET/CFP ratios are represented. p values from two-tailed Student's t tests between different samples are also represented.

the uninduced basal state while simultaneously preserving rapid and efficient membrane ruffling activation upon rapamycin addition.

In order to validate that the observed variation in basal membrane ruffling extent were as a result of different Rac1 activation levels, we further attempted to measure the Rac1 activity in these cells using a previously reported Rac1 Förster resonance energy transfer (FRET) biosensor, RaichuEV-Rac1.[13] Unfortunately, coexpression of RaichuEV-Rac1 with the heterodimerization probes system drastically compromised the expression of this molecular biosensor in Cos-7 cells, and accurate FRET measurements could not be achieved. As an alternative, we coexpressed RaichuEV-Rac1 and the heterodimerization probes in HeLa cells instead to compare the basal Rac1 activity levels in cells expressing the Golgi- and cytosol-localized Tiam1. Consistent with the membrane ruffling results, HeLa cells expressing mCherry-FKBP-Tiam1 exhibited significantly higher basal Rac1 activity than control cells expressing mCherry-FKBP, with average FRET/CFP ratios 0.56 and 0.46, respectively (MFT− vs MF−, p = 0.0243) (Figure 3c). Representative FRET/CFP cell images are shown in Supplementary Figure 5 and all statistical values are summarized in Supplementary Table S3. Importantly, the basal Rac1 activity was significantly lowered in cells when Tiam1 was prelocalized at the Golgi instead, with PH(FAPP1)-mCherry-FKBP-Tiam1-expressing cells exhibiting average FRET/CFP ratio of 0.49, comparable to that of mCherry-FKBP-expressing cells (PMFT− vs MFT−, p = 0.0407; PMFT− vs MF−, p = 0.558) (Figure 3c). Upon 7 min of rapamycin treatment, translocation of mCherry-FKBP-Tiam1 and PH(FAPP1)-mCherry-FKBP-Tiam1 to the plasma membrane resulted in a respective 1.51- and 1.49-fold increase in Rac1 activity on average (MF− vs MF+, $p < 0.001$; PMFT− vs PMFT+, $p < 0.001$), while translocation of mCherry-FKBP to the plasma

dx.doi.org/10.1021/cb300280k | ACS Chem. Biol. 2012, 7, 1950−1955

membrane did not result in a significant increase in Rac1 activity (MF− vs MF+, $p = 0.0785$). In all, we have clearly demonstrated that the prelocalization of Tiam1 at the Golgi via a defined PH(FAPP1).PI4P interaction have efficiently reduced Rac1 activity to a minimum under basal conditions, consequently maximizing the membrane ruffling output upon the chemical induction of heterodimerization.

As signaling networks in cells are being dissected more intricately, it is becoming increasingly clear that spatial and temporal control of signaling modules is the crux to regulating signal transduction of downstream events. This is especially true for the Rho family of small GTPases, which are principal regulators of cytoskeletal dynamics for various cellular functions including cell migration, adhesion, membrane trafficking, and cytokinesis.[14−16] Indeed, Rho GTPases such as Rac, Cdc42, and RhoA exhibit a highly dynamic spatiotemporal nature inside cells as revealed by fluorescent biosensors.[17,18] However, it has been a universal, inherent problem that these biosensors as well as molecular probes for manipulation of Rho GTPases exhibit background activity by either buffering or empowering physiological systems. Researchers have been circumventing these problems by carefully optimizing the expression level of the molecular probes to reduce these unwanted background signals or performing control experiments to quantify and subtract these nonspecific activities from total induced signals. Unlike these symptomatic solutions, we have improvised a spatial confinement strategy that could be adapted to reduce background signals in a variety of situations. To test the feasibility of this approach, we have demonstrated the enhanced spatiotemporal manipulation of membrane ruffling induction by a Rac1 activator. This approach relies on careful selection of two orthogonal molecular interactions occurring at two different intracellular locations: PH(FAPP).PI4P at Golgi and FKBP.rapamycin.FRB at the plasma membrane. This prelocalization scheme may be further extended to other Rho GTPases such as TC10 and additional small GTPases including K-Ras 4B, which are known to localize at the plasma membrane while having no known localization at the Golgi.[19] Nevertheless, many other small GTPases (e.g., H-Ras and Cdc42) are known to localize and have functions at the Golgi.[15,19] Therefore, the present prelocalization scheme will need to be adjusted to such circumstances for a wider use. Apart from the Golgi, additional reversible lipid−protein interactions such as PI(4,5)P2.PH-(PLCδ) at the plasma membrane[4] or PI3P.FYVE at endosomes[20] could be employed to prelocalize small GTPase molecular probes, which are then relocated to other organelles upon the addition of chemical dimerizers for small GTPase activation.

Importantly, the spatial confinement approach described here has further expanded the spatial dynamic range of chemically inducible manipulation of small GTPase activity. Molecules can now be rapidly translocated between organelles on a time scale of seconds under a physiological state. With this technique, spatiotemporal signaling is ready to be probed in greater depth.

METHODS

Cell Culture and Transfection. Cos7 or HeLa cells were cultured in DMEM (Gibco) supplemented with 10% FBS. For transfection, cells were transfected with a specified set of DNA constructs by plating them directly in a transfection solution containing DNA plasmids and FuGENE HD (Roche).

Live-Cell Microscopy. Live-cell fluorescence measurements were performed on a spinning-disk confocal microscope or the Axiovert135TV epi-fluorescence microscope (Zeiss). For confocal imaging, GFP and mCherry excitations were conducted with a krypton−argon laser (CVI-Melles Griot). The laser beam was fiber-coupled (OZ optics) to the spinning disk confocal unit (CSU10; Yokogawa) mounted with dual GFP-RFP dichroic mirrors (Semrock). The laser was processed with appropriate filter sets for GFP and mCherry (Chroma Technology) to capture fluorescence images with a CCD camera (Orca ER, Hamamatsu Photonics). Images were taken using a Neo Fluor 40× objective (Zeiss) mounted on an inverted Axiovert 200 microscope (Zeiss). For epi-fluorescence imaging, cells were imaged with a 63× oil objective (Zeiss), and images were collected by the QIClick charge-coupled device camera (QImaging). Imaging was driven by Metamorph 7.5 imaging software (Molecular Devices). Eighteen to 24 hours post-transfection, live-cell, time-lapse movies were taken where confocal fluorescent images of cells were taken every 20 s for 30 min at RT. Rapamycin (Tecoland) was added at approximately the 10 min time point. For FRET measurements, epi-fluorescence images were taken before and after 7 min of rapamycin treatment.

Fixed-Cell Microscopy. To visualize cells expressing MF, MFT, or PMFT with Golgi (CFP-Golgin), ER (CFP-Cb5), and mitochondria (CFP-Tom20) markers, cells were fixed with 4% paraformaldehyde 18 to 24 hours post-transfection, and epi-fluorescence microscopy was performed.

Quantification of Golgi Extent. CFP-Golgin was coexpressed in cells expressing MF, MFT, or PMFT to visualize Golgi structures in these cells. The Golgi spread was calculated by taking the width of Golgi stacks as a fraction of the nuclear perimeter.[11] Values presented were based on mean values collected from 22 to 39 cells.

Translocation Kinetics Measurements. Fluorescent signal intensities of fluorescence cell images and movies were measured using Metamorph 7.5 imaging software (Molecular Devices). For quantification of MF and MFT translocation kinetics, mCherry fluorescence intensity from 3 random positions in the cytosol were measured and normalized against 3 random positions in the background. For quantification of PMFT translocation kinetics, the Golgi complex was outlined, and mCherry fluorescence intensity from the highlighted region was measured; values were also normalized against a random position in the background. Translocation kinetics measurements plotted were all based on average signal intensities collected from 10 to 12 cells from 3 separate experiments. Signal intensities in Figure 2b were normalized against the highest intensity value in each case. To facilitate half-maximal translocation time calculation, graphs in Figure 2c were further scaled to a range from 0 to 1 (not shown); time duration to reach half-maximal translocation was then interpolated from these scaled translocation kinetics plots.

Quantification of Ruffle Activities. The semiquantitative scoring scheme (Supplementary Table 2) was set up to score the extent of ruffling activities exhibited by cells in the time-lapse movies. Cells were visually inspected for the extent of cellular edges displaying membrane ruffles. Membrane ruffling scores were based on average scores collected from 10 to 12 representative cells from 3 separate experiments.

FRET Measurements. To obtain the average FRET/CFP ratio of each cell, cells were first outlined, and average fluorescence intensity values were obtained from the outlined image regions in FRET and CFP channels. FRET efficiency of the Rac1 molecular biosensor in cells was then represented by respective average FRET/CFP ratios. FRET/CFP images shown have been subjected to background subtraction and color-coded according to the ratio range.

DNA Construction. We constructed mCherry-FKBP (MF) by replacing YFP of YFP-FKBP[1] with mCherry using NheI and BsrGI. To construct mCherry-FKBP-Tiam1 (MFT), we replaced YFP of YFP-FKBP-Tiam1[1] with mCherry using NheI and BsrGI. In order to construct PH(FAPP1)-mCherry-FKBP-Tiam1 (MFT), we performed PCR and amplified PH(FAPP1) with flanking restriction enzyme sites (NheI and AgeI). Both resultant product and MFT were digested with NheI and AgeI for the following ligation. Lyn-GFP-FRB was

constructed by replacing YFP of Lyn-YFP-FRB[3] with GFP using NheI and BsrGI.

Statistical Analysis. Golgi extent and RaichuEV-Rac1 FRET/CFP ratios between different samples were compared using the two-tailed Student's *t* test. Median membrane ruffling levels between different samples were compared using the two-tailed Mann−Whitney U test.

■ ASSOCIATED CONTENT

Supporting Information

This material is available free of charge via the Internet at http://pubs.acs.org.

■ AUTHOR INFORMATION

Corresponding Author

*E-mail: jctinoue@jhmi.edu.

Notes

The authors declare no competing financial interest.

■ ACKNOWLEDGMENTS

We thank T. Balla (NIH) for a FAPP-PH construct and K. Aoki and M. Matsuda (Kyoto University) for a RaichuEV-Rac1 construct. This study was supported in part by National Institutes of Health (MH084691 and GM092930 to T.I.). S.C.P. is a recipient of the National Science Scholarship from Agency for Science, Technology and Research (Singapore).

■ REFERENCES

(1) Inoue, T., Heo, W. D., Grimley, J. S., Wandless, T. J., and Meyer, T. (2005) An inducible translocation strategy to rapidly activate and inhibit small GTPase signaling pathways. *Nat. Methods 2*, 415−418.

(2) Miyamoto, T., DeRose, R., Suarez, A., Ueno, T., Chen, M., Sun, T. P., Wolfgang, M. J., Mukherjee, C., Meyers, D. J., and Inoue, T. (2012) Rapid and orthogonal logic gating with a gibberellin-induced dimerization system. *Nat. Chem. Biol. 8*, 465−470.

(3) Komatsu, T., Kukelyansky, I., McCaffery, J. M., Ueno, T., Varela, L. C., and Inoue, T. (2010) Organelle-specific, rapid induction of molecular activities and membrane tethering. *Nat. Methods 7*, 206−208.

(4) Ueno, T., Falkenburger, B. H., Pohlmeyer, C., and Inoue, T. (2011) Triggering actin comets versus membrane ruffles: distinctive effects of phosphoinositides on actin reorganization. *Sci. Signal. 4*, 87.

(5) DeRose, R., Pohlmeyer, C., Umeda, N., Ueno, T., Nagano, T., Kuo, S., and Inoue, T. (2012) Spatio-temporal manipulation of small GTPase activity at subcellular level and on timescale of seconds in living cells. *J. Vis. Exp. 9*, 3794.

(6) Umeda, N., Ueno, T., Pohlmeyer, C., Nagano, T., and Inoue, T. (2011) A photocleavable rapamycin conjugate for spatiotemporal control of small GTPase activity. *J. Am. Chem. Soc. 133*, 12−14.

(7) Haruki, H., Nishikawa, J., and Laemmli, U. K. (2008) The anchor-away technique: rapid, conditional establishment of yeast mutant phenotypes. *Mol. Cell 31*, 925−932.

(8) Varnai, P., and Balla, T. (2007) Visualization and manipulation of phosphoinositide dynamics in live cells using engineered protein domains. *Pflugers Arch. 455*, 69−82.

(9) Stahelin, R. V., Karathanassis, D., Bruzik, K. S., Waterfield, M. D., Bravo, J., Williams, R. L., and Cho, W. (2006) Structural and membrane binding analysis of the Phox homology domain of phosphoinositide 3-kinase-C2alpha. *J. Biol. Chem. 281*, 39396−39406.

(10) Banaszynski, L. A., Liu, C. W., and Wandless, T. J. (2005) Characterization of the FKBP.rapamycin.FRB ternary complex. *J. Am. Chem. Soc. 127*, 4715−4721.

(11) Dippold, H. C., Ng, M. M., Farber-Katz, S. E., Lee, S.-K., Kerr, M. L., Peterman, M. C., Sim, R., Wiharto, P. A., Galbraith, K. A., Madhavarapu, S., Fuchs, G. J., Meerloo, T., Farquhar, M. G., Zhou, H., and Field, S. J. (2009) GOLPH3 bridges phosphatidylinositol-4-phosphate and actomyosin to stretch and shape the golgi to promote budding. *Cell 139*, 337−351.

(12) Ihara, S., Oka, T., and Fukui, Y. (2006) Direct binding of SWAP-70 to non-muscle actin is required for membrane ruffling. *J. Cell Sci. 119*, 500−507.

(13) Komatsu, N., Aoki, K., Yamada, M., Yukinaga, H., Fujita, Y., Kamioka, Y., and Matsuda, M. (2011) Development of an optimized backbone of FRET biosensors for kinases and GTPases. *Mol. Biol. Cell 22*, 4647−4656.

(14) Etienne-Manneville, S., and Hall, A. (2002) Rho GTPases in cell biology. *Nature 420*, 629−635.

(15) Pertz, O. (2010) Spatio-temporal Rho GTPase signaling: where are we now? *J. Cell Sci. 123*, 1841−1850.

(16) Takai, Y., Sasaki, T., and Matozaki, T. (2001) Small GTP-binding proteins. *Physiol. Rev. 81*, 153−208.

(17) Itoh, R. E., Kurokawa, K., Ohba, Y., Yoshizaki, H., Mochizuki, N., and Matsuda, M. (2002) Activation of rac and cdc42 video imaged by fluorescent resonance energy transfer-based single-molecule probes in the membrane of living cells. *Mol. Cell. Biol. 22*, 6582−6591.

(18) Pertz, O., Hodgson, L., Klemke, R. L., and Hahn, K. M. (2006) Spatiotemporal dynamics of RhoA activity in migrating cells. *Nature 440*, 1069−1072.

(19) Michaelson, D., Silletti, J., Murphy, G., D'Eustachio, P., Rush, M., and Philips, M. R. (2001) Differential localization of Rho Gtpases in live cells. *J. Cell Biol. 152*, 111−126.

(20) Zoncu, R., Perera, R. M., Balkin, D. M., Pirruccello, M., Toomre, D., and De Camilli, P. (2009) A phosphoinositide switch controls the maturation and signaling properties of APPL endosomes. *Cell 136*, 1110−1121.

■ NOTE ADDED AFTER ASAP PUBLICATION

This paper was published ASAP on September 25, 2012. Reference 13 has been changed. The revised version was posted on October 8, 2012.